PACE-2021
International Congress on the Phenomenological Aspects of Civil Engineering

Research Article 20-23 June 2021

Buckling of cylindrical shells with stepwise wall thickness subjected to combined loading

Neda Fazlalipour*,[1] Hossein Showkati[1], Saeed Eyvazinejad Firouzsalari[2]

[1] *Department of Civil Engineering, Urmia University, Urmia, Iran*
[2] *Department of Civil and Environmental Engineering, The University of Auckland, New Zealand*

Corresponding Author Email: n.fazlalipour@urmia.ac.ir *Corresponding Author ORCID: 0000-0002-1764-0974*

Keywords

Cylindrical shell,
Tank,
Stepwise wall thickness,
Buckling,
Combined loading.

Abstract

An experimental, numerical, and theoretical study was conducted to investigate the buckling behaviour of cylindrical shells with stepwise wall thickness when subjected to a combination of axial compression preloading and external pressure. The effect of axial pre-compression on the buckling load, buckling mode of the cylindrical shell were evaluated. Additionally, numerical modelling was employed to verify the experimental results and relationships available in the design codes for predicting the buckling load of cylindrical shells with a uniform wall thickness were modified to for cylindrical shells with stepwise wall thickness. Comparable predictions between the modified analytical and numerical models and the experiment were observed.

1.Introduction

Cylindrical steel shells are industrial structures that play an important role in the storage of petroleum and refineries, potable water supply and fire extinguishing systems [1–3]. Steel storage cylindrical shells are manufactured with variable thicknesses in height for economic reasons. Each cylindrical shell structure is made from several individual cylindrical shells of constant thickness, with the wall thickness increasing progressively from top of the shell to the bottom [4–6]. These shells with fixed roofs are subject to axial pressure due to snow accumulating on the roof. Shells are subjected to external pressure due to wind load or when the containing liquid is discharged, with the combination of axial compression and external pressure could conclude the structural failure of the shells [7–12].

Brush and Almroth (1975) [13] proposed an equation to predict the buckling load of steel cylindrical shells with a uniform wall thickness. Hutchinson (1965) [14] showed that the geometric imperfections significantly reduced the buckling load of the steel cylindrical shells with a uniform wall thickness. Shen and Chen (1991) [15] and Pourkhorshidi and Abedi (2017) [16] showed the significant effect of the combined load proportions, cylindrical shell geometry, and the geometrical imperfections on the buckling load of the cylindrical shells. Naserkhani and Epakchi (2019) [17] proposed a relationship that closely predicted the buckling load of cylindrical shells with non-uniform wall thickness subjected to combined axial compression and external pressure.

A review of previous research in cylindrical shell buckling shows that the effect of stepwise wall thickness on the buckling behaviour of cylindrical shells subjected to combined axial compression and external pressure has received markedly little appraisal. In the reported study, it was assumed that a cylindrical shell carries axial compression and is then subjected to external pressure. The effect of axial pre-compression on the buckling load and buckling mode of cylindrical shells with stepwise wall thickness are evaluated using Finite Element (FE) numerical modelling and theoretically.

2. Testing process

2.1. Specimen manufacture

A cylindrical shell was manufactured from three individual cylindrical shell sections with radius of 300 mm, height of 150 mm and thickness of 0.3, 0.4 and 0.5 mm such that the thickness of the individual cylindrical shells increased stepwise downwards. The edges of individual cylindrical shells were welded together using strips with dimensions of 10×0.3 mm2 and Spot Welding system (see Fig. 1a). The welded areas were sealed from the external surface of the shell using silicone sealant. The dimensions of the cylindrical shell are shown in Figure 1b.

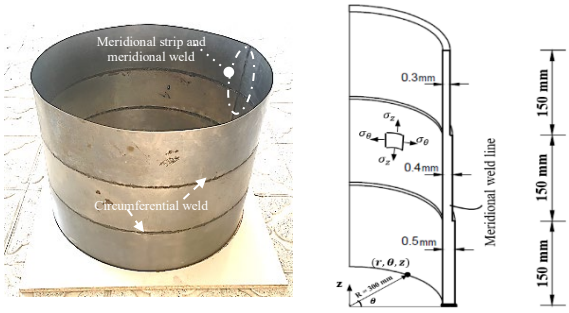

(a) Circumferential and meridional welds (b) Dimensions of specimen

Figure 1. Dimensions and manufacturing process of cylindrical shell.

2.2. Test setup

The cylindrical shell was placed between rigid plates at the top and the bottom with the edges of the cylindrical shell was constrained against any radial displacement by positioning in the grooves provided in the rigid plates. The edges of the shell were sealed against any air leakage using gasket glues. Axial pre-compression was applied to the cylindrical shell using a vertical jack and external pressure loading was applied using a vacuum pump. Four digital dial indicators were used to measure shell vertical and radial displacements at different locations on the shell surface. The coordinates of the instruments given in Table 1.

Three tensile tests were performed on coupon samples that were produced from the steel sheets with varying thicknesses, according to ASTM-E8m [18], and the stress-strain diagrams for average of three tensile tests are shown in Figure 3.

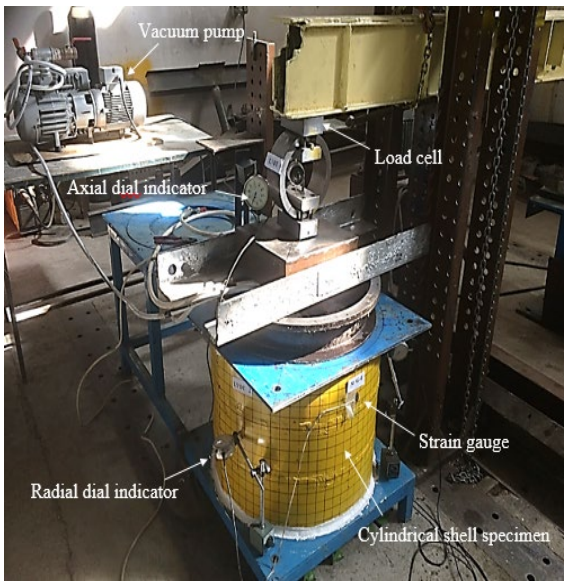

Figure 2. Overall view of the test set-up.

Table 1. Location of the LVDTs on specimen.

Instrument	θ (degree)	Z (mm)
Dial indicator 1	---*	450
Dial indicator 2	20	255
Dial indicator 3	145	345
Dial indicator 4	240	345

*Dial indicator 1 was located on the top rigid plate.

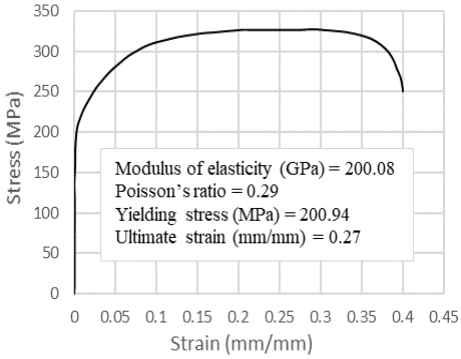

Figure 3. Stress-strain relationship of cylindrical shell material.

3. Test results

The test procedure involved first applying axial pre-compression to the top edge of the shell specimen up to 1.78 kN and then applying the external pressure by discharging the air inside the shell while keeping the value of the axial compression constant. In Fig. 4a, the axial pre-compression versus radial displacement are shown, and in Fig. 4b, the total axial compression (axial pre-compression plus additional axial compression derived from external pressure application)-displacement relationships are depicted. Dial indicator 2 to 4 showed shell radial displacement while dial indicator 1 recorded shell vertical displacement at the axial compression load location. Fig. 4a shows insignificant deformation of the cylindrical shell when subjected to axial compression, however, with an application of external pressure shell deformation increased up to P = 2.58 kPa at which shell initial circumferential buckling occurred. Further increase in the external pressure caused an increase in the vertical and radial shell displacement until the shell buckling was achieved at an external pressure equal to P = 4.73 kPa, which was associated with larger shell radial displacement as shown in Fig. 4c.

The shell specimens failed due to the development of circumferential waves (see fig. 5) with the starting point of the initial circumferential buckling wave marked in Fig. 4b and Fig. 4c. Further external pressure caused the development of circumferential half-sine waves in the form of inward deformation separated by vertical crests (Fig. 5), with the number of the developed waves increasing with an increase in the external pressure. The cylindrical shell failed at an external pressure equal to P = 4.73 kPa at which ten half-sine waves were detected.

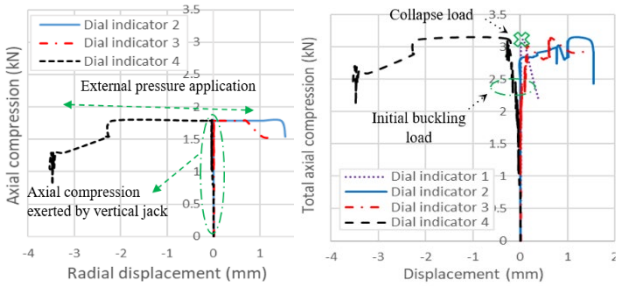

(a) Axial compression-radial displacement relationships

(b) Total axial compression-displacement relationships

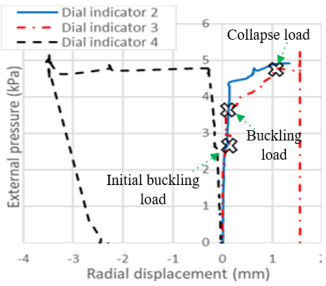

(c) external pressure-radial displacement relationships

Figure 4. Experimental curves relationship of cylindrical shells.

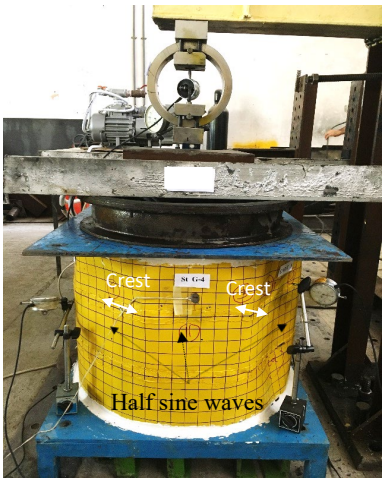

Figure 5. After-test configuration of shell specimen.

4. Numerical modelling

General-purpose finite element (FE) program ABAQUS [19] was used to simulate the test. The shell specimen and the boundary conditions were modelled using the geometric properties of the test specimen and the test set-up (see Fig. 1b and Fig. 6), and the material properties were modelled using true stress-strain relationships. The strips were connected to the individual cylindrical shells using the tie option (see Fig. 6). Top and bottom rigid plates were not modelled to simplify the FE model and to reduce the analysis time. The first buckling mode, obtained from eigenvalue buckling analysis, was used as initial geometric imperfection for models, similar to methods used in Refs.[7,19,20]. The size of the maximum geometric imperfection obtained from the specimen was 0.5 mm, therefore, a scale factor of 0.5 was considered for the first buckling mode in FE analysis. Two steps are defined to simulate the experimental loading stages including (i) nonlinear general static analysis for modelling the axial pre-compression in the form of linear distributed load applied on the top edge of the model (p), and (ii) Riks analysis for applying external pressure to trace unstable equilibrium paths that may exhibit 'snap-through' or 'snap-back' [21,22]. The additional axial compressive stresses due to the external pressure was modelled as a function of the external pressure and perimeter of the shell cross-section ((πR^2)/2πR) and applied to the top edge of the model (see Fig. 6). The cylindrical shell was modelled using four-node, three-dimensional and doubly curved shell element S4R having a mesh of 10 mm elements.

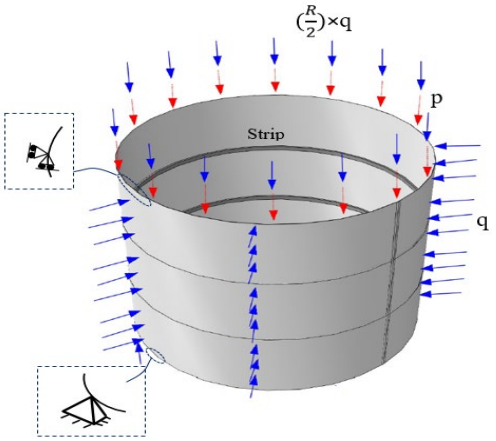

Figure 6. Details of FE model.

5. Verification of numerical simulation

In Figure 7, external pressure versus radial displacement relationships at dial indicator locations for the tested specimen were compared with the associated numerical model. Additionally, the collapse load and the number of circumferential waves obtained from experiment and numerical modelling are listed in Table 2. The results indicated that there was a close correlation between the experimental and the FE results. There were small discrepancies between the experimental and FE graphs in Fig. 7 mainly due to several un-modelled parameters such as support conditions in the FE model that did not exactly represent the test set-up, residual stresses.

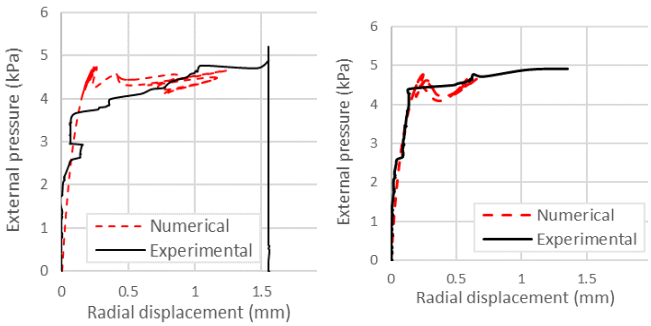

(a) Dial indicator 1 (b) Dial indicator 2

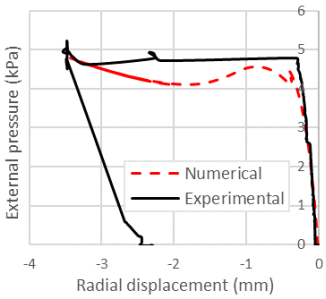

(c) Dial indicator 3

Figure 7. Comparison of experimental and FE results for external pressure-radial displacement relationships of cylindrical shells.

Table 2. compaction of experimental and numerical results.

specimen	Axial compression (kN)	Collapse load (kPa)	Number of wave	Eror (%)
Experiment	1.78	4.73	10	1.05
FE model	1.78	4.78	9	

Four scale factors equal to 0 (no imperfection), 0.25, 0.50, and 0.75 were used to evaluate the effect of the initial geometric imperfections on the buckling load of the stepwise cylindrical shells. Ten cylindrical shells with similar geometry that had varying axial pre-compressions were modelled for each specific value of scale factor, and axial compression-external pressure interaction graphs were depicted in Fig. 8, with the results indicating that the buckling load decreased with increasing the scale factor.

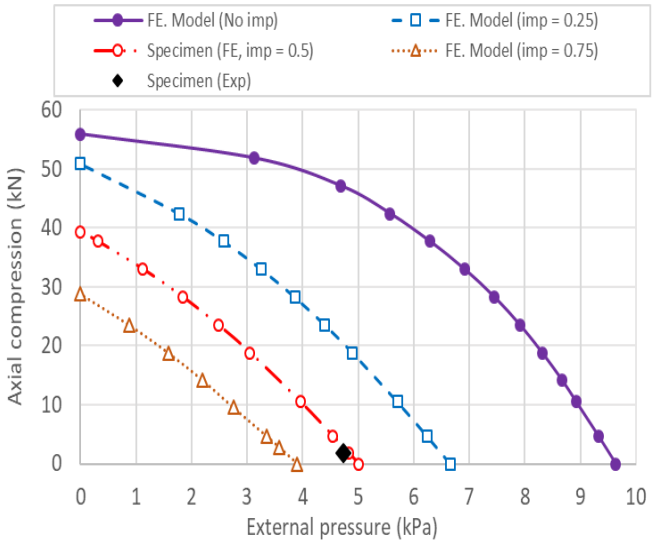

Figure 8. Interaction curve of axial compression-external pressure.

6. Comparison of theoretical and numerical results

In EN 1993-1-6 [23], the buckling load of cylindrical shells with stepwise wall thickness subjected to external pressure was calculated first by dividing the shell height to three fictitious individual sections with a specific length and wall thickness. In the next step, the cylindrical shell that has three fictitious individual cylindrical shells is replaced with an equivalent cylindrical shell with a uniform wall thickness equal to t_a (Eq. 1) and an effective length of l_{eff} (Eq. 2), [24] which is determined by:

$$t_a = \frac{1}{l_a}\sum_a l_j t_j \quad (1)$$

$$l_{eff} = \frac{l_a}{k} \quad (2)$$

where l_a is the height of the top section and k is a dimensionless factor indicating the stiffness effect of the bottom sections and is determined using the graphs that were provided in EN 1993-1-6 [23]

Chen et al. [4] proposed a theoretical relationship for determining the equivalent wall thickness of cylindrical shells with a stepwise wall thickness subjected to external pressure using weight distribution and based on energy principles (Eq. 3):

$$t_{eq}^3 = \left(\frac{1}{l'_{eff}}\right)\sum_{i=1}^{n}[t_i^3(\chi_i - \chi_{i-1})]. \quad i = 1,2,\dots,n \quad (3)$$

$$\chi_i = \left(h_i - \frac{l'_{eff}}{2\pi} sin\ \frac{2\pi h_i}{l'_{eff}}\right) \quad (4) \quad (4)$$

in which l_{eff} is the effective length of the cylindrical shell, and h_i is the distance from the top of the shell to the bottom of the ith section, Note that in Eqs 3 and 4 for $i = 1$, then $h_0 = 0$ and $\chi_0 = 0$.
Brush et al. [13] proposed a theoretical relationship to predict the buckling load of cylindrical shells with a uniform wall thickness and simple boundary conditions subjected to a combination of axial compression (N) and a uniform external pressure (q) as below:

$$q = \frac{(\underline{m}^2+n^2)^4\left(\frac{D}{R^2}\right)+\underline{m}^4(1-\nu^2)C}{R(\underline{m}^2+n^2)^2(n^2+K\underline{m}^2)} \quad (5)$$

$$C = \frac{Et}{(1-\nu^2)} \quad (6)$$

$$D = \frac{Et^3}{12(1-\upsilon^2)} \quad (7)$$

$$\underline{m} = \frac{m\pi R}{l} \quad (8)$$

in which K is a load ratio and is defined as a unique eigenvalue corresponding to each pair of m and n values, which is calculated by [13]:

$$\frac{N}{2\pi R} = KqR \quad (9)$$

where t is the shell wall thickness, E is Young's modulus, R is the radius of the cylindrical shell, l is the buckling length, n is the number of circumferential waves, m is the number of longitudinal waves, and υ is the Poisson's ratio.

For the tested specimen, the equivalent wall thickness and the effective length were calculated using the equations by Eq. 1 and Eq. 3 that are given in Table 3.

Table 3. Equivalent wall thickness and effective length of cylindrical shell specimen.

	D (mm)	Ref. [4]		Ref. [23]	
		L_{eff} (mm)	t_{eq} (mm)	L_{eff} (mm)	t_{eq} (mm)
Specimen	600	307.50	0.36	300	0.33

Then, the external pressures (q) that caused buckling were calculated using Eq. 5 and compared with the FE results in Table 4 and in Fig. 9.

Table 4. Comparison of theoretical predictions with numerical results.

Axial compression (kN)	Buckling load	Prediction by Eq. 5			
	FE analyses (kPa)	L_{eff} & t_{eq} based on Ref. [4]		L_{eff} & t_{eq} based on Ref. [23]	
		Value (kPa)	Error (FE)%	Value (kPa)	Error (FE)%
0	9.64	9.37	2.80	7.88	18.25
4.71	9.32	8.97	3.75	7.51	19.42
10.47	8.92	8.47	5.04	7.07	20.74
14.13	8.67	8.17	2.88	6.75	22.14
18.85	8.31	7.77	6.50	6.34	23.71
23.56	7.91	7.37	6.83	5.92	25.16

28.27	7.45	6.97	6.44	5.50	26.17
32.98	6.91	6.57	4.92	5.08	26.48
37.70	6.29	6.17	1.90	4.66	25.91
42.41	5.57	5.72	2.69	4.24	23.87
47.12	4.69	5.26	10.84	3.82	18.55
51.84	3.12	4.80	53.84	3.38	8.33
55.88	0	4.40	-	2.96	-

The effect of geometric imperfections was not considered in Eq. 5; thus, the theoretical predictions were compared with the results of FE analysis in which no geometric imperfections were modelled.

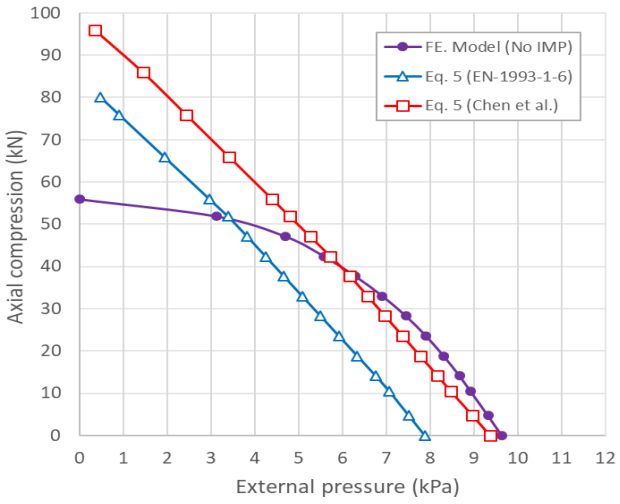

Figure 9. Interaction curve of axial pre-compression-external pressure for Comparison of theoretical predictions with numerical results.

In Figure 9 interaction curves for axial compression and external pressure obtained from numerical analysis and Eq. 5 are shown. The graph obtained from Eq. 5 was linear because imperfections were neglected in this equation [15]. In FE analysis, however, the interaction graph was non-linear due to nonlinear geometric modelling of the shell materials. for axial compression values smaller than 47 kN, Eq. 5, in which t_{eq} and l_{eff} were calculated using the method proposed by Chen et al. [4], gave a better prediction of the FE results (maximum deviation 10%) when compared to the situation where t_{eq} and l_{eff} were calculated using Eqs. 1 and 2. The reason for this deviation was mainly attributed to the differences in support conditions in the FE model and the theoretical assumptions. Additionally, for larger values of axial pre-compression, the top individual shell that had the smallest wall thickness failed earlier than the individual shells with larger wall thickness.

7. Conclusions

In this study, the buckling behaviour of cylindrical shells with stepwise wall thickness (three individual cylindrical shells) when subjected to a combination of axial pre-compression and external pressure was investigated experimentally, numerically and theoretically. Vertical and radial displacements of the shell were recorded and axial compression vs external pressure interaction graphs were obtained. Conclusions drawn are listed as follows:

- With decreasing the axial compression value, the buckling mode of the tested specimens were akin to the buckling mode of cylindrical shells subjected to pure external pressure.
- The numerical simulation method employed in the current study can be used to predict the buckling load of cylindrical shells with stepwise wall thickness.
- The buckling load of the cylindrical shells decreased with increasing the value of the geometric imperfection.
- The modified versions of analytical models proposed by Chen et al. [4] gave a better prediction of the FE results.
- With increasing the value of axial pre-compression, the individual shell with the smallest wall thickness failed earlier than other individual shells that had larger wall thickness.

Declaration of Conflict of Interests

The authors declare that there is no conflict of interest. They have no known competing financial interests or personal relationships.

References

[1.] J. de WIT, Steel Vertical Cylindrical Storage Tanks, Butterworth & Co (Publishers) Ltd, 1973. https://doi.org/10.1016/b978-0-408-00083-3.50030-8.
[2.] M. Yazdanian, S.E. Firouzsalari, J. Ingham, D. Dizhur, M. Yazdanian, S.E. Firouzsalari, J. Ingham, D. Dizhur, Stability of Beams View project Observations and Categorisation of Building Envelopes After Being Subjected to Earthquakes and Suggested Improvements to Existing Testing Protocols View project, n.d. https://www.researchgate.net/publication/351102965.
[3.] E. Azzuni, S. Guzey, Comparison of the shell design methods for cylindrical liquid storage tanks, Eng. Struct. 101 (2015) 621–630.
[4.] L. Chen, J. Michael Rotter, C. Doerich, Buckling of cylindrical shells with stepwise variable wall thickness under uniform external pressure, Eng. Struct. 33 (2011) 3570–3578. https://doi.org/10.1016/j.engstruct.2011.07.021.
[5.] M. Maali, A.C. Aydın, H. Showkati, M. Sağıroğlu, M. Kılıç, The effect of longitudinal imperfections on thin-walled conical shells, J. Build. Eng. 20 (2018) 424–441. https://doi.org/10.1016/j.jobe.2018.08.005.
[6.] Z. Chen, L. Yang, G. Cao, W. Guo, Buckling of the axially compressed cylindrical shells with arbitrary axisymmetric thickness variation, Thin-Walled Struct. 60 (2012) 38–45.
[7.] L.A. Godoy, Buckling of vertical oil storage steel tanks: Review of static buckling studies, Thin-Walled Struct. 103 (2016) 1–21. https://doi.org/10.1016/j.tws.2016.01.026.
[8.] R.C. Jaca, L.A. Godoy, J.G.A. Croll, Reduced Stiffness Buckling Analysis of Aboveground Storage Tanks with Thickness Changes, n.d. https://journals.sagepub.com/doi/abs/10.1260/1369-4332.14.3.475 (accessed December 2, 2020).
[9.] L. Yang, Z. Chen, F. Chen, W. Guo, G. Cao, Buckling of cylindrical shells with general axisymmetric thickness imperfections under external pressure, Eur. J. Mech. 38 (2013) 90–99.
[10.] S. Eyvazinejad Firouzsalari, H. Showkati, J.M. Ingham, Free-spanning and base-supported tubes subjected to combined axial compression and indentation loads, J. Constr. Steel Res. 161 (2019) 341–354. https://doi.org/10.1016/j.jcsr.2019.07.001.
[11.] R. Naseri Ghalghachi, H. Showkati, S. Eyvazinejad Firouzsalari, Buckling behaviour of GFRP cylindrical shells subjected to axial compression load, Compos. Struct. 260 (2021) 113269. https://doi.org/10.1016/j.compstruct.2020.113269.
[12.] S.E. Firouzsalari, H. Showkati, Investigation of free-spanned pipeline behavior due to axial forces and local loads, J. Constr. Steel Res. 86 (2013) 128–139. https://doi.org/10.1016/j.jcsr.2013.03.018.
[13.] D.O. Brush, W.L. Jolly, O.D. Brush, B.O. Almroth, Buckling of Bars, Plates, and Shells, McGraw-Hill, 1975. https://books.google.com/books?id=k1bQAQAACAAJ.
[14.] J. Hutchinson, Buckling of imperfect cylindrical shells under axial compression and external pressure, AIAA J. 3 (1965) 1968–1970. https://doi.org/10.2514/3.3299.
[15.] H. Shen, T. Chen, Buckling and postbuckling behaviour of

cylindrical shells under combined external pressure and axial compression, Thin-Walled Struct. 12 (1991) 321–334. https://doi.org/https://doi.org/10.1016/0263-8231(91)90032-E.
[16.] S. Pourkhorshidi, K. Abedi, 05.16: Stability behavior of graded dented cylindrical steel shells under the action of combined external and axial pressure, Ce/Papers. 1 (2017) 1162–1171. https://doi.org/10.1002/cepa.157.
[17.] F. Mahboubi Nasrekani, H. Eipakchi, Analytical solution for buckling analysis of cylinders with varying thickness subjected to combined axial and radial loads, Int. J. Press. Vessel. Pip. 172 (2019) 220–226. https://doi.org/10.1016/j.ijpvp.2019.03.036.
[18.] ASTM Standard E8/E8M-13a, "Standard Test Methods for Tension Testing of Metallic Materials," 2013. https://doi.org/10.1520/E0008_E0008M-13A.
[19.] (PDF) ABAQUS/CAE User's Manual ABAQUS/CAE User's Manual | PYLA NARENDRA NAIDU ce14b097 - Academia.edu, (n.d.). https://www.academia.edu/38631701/ABAQUS_CAE_Users_Manual_ABAQUS_CAE_Users_Manual (accessed August 26, 2020).
[20.] üS.S.S. Aly, Buckling Assessment of Axially Loaded Cylindrical Shells with Random Imperfections, Iowa State University, 1995. https://books.google.com/books?id=ryratgAACAAJ.
[21.] üS.E. Firouzsalari, H. Showkati, Thorough investigation of continuously supported pipelines under combined pre-compression and denting loads, Int. J. Press. Vessel. Pip. 104 (2013) 83–95. https://doi.org/https://doi.org/10.1016/j.ijpvp.2013.01.008.
[22.] üS. Eyvazinejad Firouzsalari, H. Showkati, Behavior of pre-compressed tubes subjected to local loads, Ocean Eng. 65 (2013) 19–31. https://doi.org/https://doi.org/10.1016/j.oceaneng.2013.03.003.
[23.] üEN 1993-1-6: Eurocode 3: Design of steel structures - Part 1-6: Strength and stability of shell structures, 1993.
[24.] üP. Taraghi, H. Showkati, S.E. Firouzsalari, The performance of steel conical shells reinforced with CFRP laminates subjected to uniform external pressure, Constr. Build. Mater. 214 (2019) 484–496. https://doi.org/10.1016/j.conbuildmat.2019.04.015.